Tunable add/drop channel coupler based on an acousto-optic tunable filter and a tapered fiber

Wending Zhang,[1] Ligang Huang,[1] Feng Gao,[1,*] Fang Bo,[1] Li Xuan,[2] Guoquan Zhang,[1,3] and Jingjun Xu[1,2]

[1]*MOE Key Laboratory of Weak-Light Nonlinear Photonics, TEDA Applied Physics School and School of Physics, Nankai University, Tianjin 300457, China*

[2]*State Key Laboratory of Applied Optics, Changchun Institute of Optics, Fine Mechanics and Physics, Chinese Academy of Sciences, Changchun 130033, China*

[3]*e-mail: zhanggq@nankai.edu.cn*

**Corresponding author: fenggao@nankai.edu.cn*

Received November 24, 2011; revised January 2, 2012; accepted February 15, 2012; posted February 23, 2012 (Doc. ID 158509); published March 28, 2012

We report a tunable add/drop channel coupler based on an acousto-optic tunable filter and a tapered fiber. The coupling efficiency and central wavelength of the add/drop channel coupler are tunable by simply tuning the power and frequency of the driving radio frequency signal. Further possible improvements on the configuration are also discussed. © 2012 Optical Society of America

OCIS codes: 060.2310, 060.2430, 060.2330, 060.2280.

In recent years, the add/drop channel coupler has attracted much attention [1] because of its potential applications in wavelength-division-multiplexing (WDM) systems [2], which is one of the most important components for enhancing the efficiency and flexibility of the fiber communication network. Early studies on the add/drop channel coupler focused mainly on the incorporation of fiber Bragg gratings (FBGs) to achieve wavelength selectivity [3–4]. Because the FBG device has to be operated in the reflection mode [5], it may introduce unwanted optical feedback and extra loss in retrieving the reflected signal. Subsequently, a component composed of two parallel identical long-period fiber grating (LPFG) was introduced into the add/drop channel coupler [6–7], and it was operated in the transmission mode and did not have problems in the reflection mode [8]. Besides, there were also other configurations for the add/drop channel coupler, for example, the combination of the LPFG with either the FBG [9] or the tapered fiber [10]. However, it was difficult for the above configurations to control effectively the spectral characteristics such as the coupling efficiency and, more importantly, the central wavelength of the add/drop channel coupler. The most recent work with controllable spectral parameters was based on two parallel identical LPFGs with voltage-controllable coil heaters [11]. In this Letter, we report a tunable add/drop channel coupler based on an acousto-optic tunable filter (AOTF) and a tapered fiber. The output of the AOTF shows the band-rejection characteristic, and the output of the tapered fiber shows the bandpass characteristic. The coupling efficiency and the central wavelength of the add/drop channels could be adjusted by tuning the power and frequency of the driving radio frequency (RF) signal applied to the AOTF. At the same time, possible improvements on the configuration were also discussed.

It is known that the AOTF is composed of an acoustic wave generation system and an unjacketed single-mode fiber (SMF) [12]. When the acoustic wave propagates along the unjacketed SMF, a periodic modulation of the refractive index is produced with a period of hundreds of micrometers in the core of the unjacketed SMF, and such a core refractive index modulation would induce a mode-coupling between the core fundamental mode (LP_{01}^{co}) and the copropagation cladding modes (LP_{1u}^{cl}) when the phase matching condition is satisfied [13]:

$$\lambda = \left(n_{01}^{co} - n_{1u}^{cl}\right)\Lambda, \tag{1}$$

where λ is the central wavelength; n_{01}^{co} and n_{1u}^{cl} are the effective index of the core and cladding modes, respectively; and Λ is the acoustic wavelength in the unjacketed SMF. As a result, the nonresonant mode propagates in the core and the resonant mode propagates in the cladding of the AOTF. Thus, the mode coupling between them generates a notch in the transmission spectrum of the AOTF. If a tapered fiber with its uniform waist part is close enough to the AOTF right after the acousto-optic (AO) interaction region of the AOTF (see Fig. 1), the cladding mode in the AOTF can be coupled to the cladding mode of the tapered fiber via an evanescent wave. The cladding mode in the uniform waist part of the tapered fiber will be coupled to its core mode through a transition zone with its diameter increasing exponentially up to that of the tail fiber and then propagating along the tapered fiber [14]. Therefore, the nonresonant and resonant modes can be separated and directed to the outputs of the AOTF and the tapered fiber, respectively. The output of the AOTF (Port 2) would show the band-rejection characteristic, and that of the tapered fiber (Port 3)

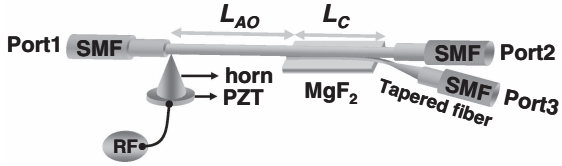

Fig. 1. Experimental configuration of the tunable add/drop channel coupler: L_{AO}, length of AO interaction region; L_C, length of the evanescent wave coupling region supported by a low-index MgF_2 substrate and dipped into a refractive-index-matched liquid.

 © 2012 Optical Society of America

would show the bandpass characteristic; i.e., the structure works as an add/drop channel coupler. In addition, the coupling efficiency and the central wavelength of the output signals can be adjusted by tuning the power and frequency of the driving RF signal applied to the AOTF.

Figure 1 is the experimental configuration of the tunable add/drop channel coupler. The structure of the AOTF was the same as that in a previous work we reported [15]. An axial mode piezoelectric transducer (PZT) was attached to a cone acoustic transducer, and the other side of it was attached to a steel plate as a mount. The unjacketed SMF had a step index of $\Delta = 0.32\%$, with a core radius of $\rho_{co} = 4.5$ μm and a cladding radius of $\rho_{cl} = 62.5$ μm. The outer diameter of the SMF was etched down to 30 μm by the hydrofluoric acid, and the length of the etched region was 38 mm. The uniform waist part of the tapered fiber was fabricated with a diameter of 18 μm and a length of 14 mm, and the transition zone of the tapered fiber was 5 mm. The uniform waist part of the tapered fiber was attached along the etched SMF of the AOTF with a coupling length of $L_C = 10$ mm. To increase the coupling efficiency, the coupling region was dipped into a refractive-index-matched liquid ($n = 1.450$), where the acoustic wave was absorbed and therefore the AO interaction length L_{AO} was limited to 28 mm. The whole coupling region was supported by a piece of MgF_2 substrate with a lower refractive index of ~1.37.

RF power of 0.4 dBm was applied to the PZT at a frequency of 0.850 MHz. With an unpolarized light from a broadband light source coupled into Port 1 of the SMF, the transmission spectra of Ports 2 and 3 were measured. The experimental results are presented in Fig. 2. The black solid curve denotes the transmission spectrum of Port 2, and it shows a band-rejection characteristic with a peak efficiency of −17.1 dB at the central wavelength 1562.7 nm due to the mode coupling between the LP_{01}^{co} and LP_{11}^{cl} modes. The red dashed curve denotes the transmission spectrum of Port 3, showing a bandpass characteristic with peak efficiency of −5.1 dB. The two measured spectra are complementary with each other. Furthermore, by coupling the light into Port 3, i.e., adding the signal to the SMF via the tapered fiber, the output spectrum of Port 1 was measured and depicted as the blue dashed–dotted curve in Fig. 2. One sees that the blue dashed–dotted curve coincides with the red dashed curve, which means that the signal adding and dropping are almost of the same loss of −5.1 dB. Note that the bandwidth of the add/drop channels could be narrowed by increasing the AO interaction length L_{AO} [16].

With the light coupling into Port 1, the spectral tunability of Port 3 is presented in Fig. 3. By increasing the RF driving power from −9.6 dBm to 0.4 dBm at 0.850 MHz, the peak bandpass coupling efficiency of Port 3 can be adjusted from −13 to −5.1 dB at the same central wavelength of 1562.7 nm, as shown in Fig. 3(a). Furthermore, the spectral central wavelength of the Port 3 is blue-shifted linearly with a tuning slope of −0.88 nm/kHz when one increases the driving RF frequency. For example, the central wavelength of Port 3 can be tuned from 1594.7 to 1539.8 nm, covering both the C and L bands, when the RF frequency is tuned from 0.820 to 0.880 MHz, as shown in Fig. 3(b). Meanwhile, the spectral central wavelength of Port 3 is always in coincidence with that of Port 2.

With this configuration, the coupling efficiency and the central wavelength of the add/drop channels can be adjusted quickly and easily [7,10]. Furthermore, it is easy to incorporate into optical communication systems because of its all-SMF structure [13].

The above experimental results have demonstrated the feasibility of the configuration. Moreover, the bandpass coupling efficiency can be increased further on to reduce the loss of the signal, which is very important for practical applications of optical communication [7,10,11]. A theoretical calculation based on the experiment [17] shows that the bandpass coupling efficiency depends on the coupling length L_C in a significant way. The bandpass coupling efficiency reaches a maxima at a coupling length of $L_C = 15$ mm, as shown by the solid curve in Fig. 4. The coupling length L_C can be finely adjusted in the experiments with a translation stage under the monitoring of a stereomicroscope. The relationship between the bandpass coupling efficiency and L_C was measured experimentally, and the results are shown by the solid squares in Fig. 4. One sees that the experimental

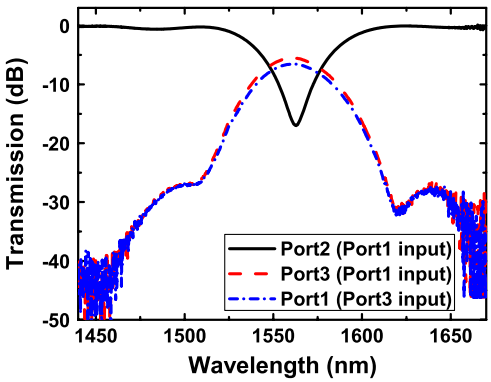

Fig. 2. (Color online) The black solid and red dashed curves denote the output spectra of Ports 2 and 3, respectively, when coupling the light into Port 1. The blue dashed–dotted curve denotes the output spectrum at Port 1 of the AOTF by coupling the light into the tapered fiber.

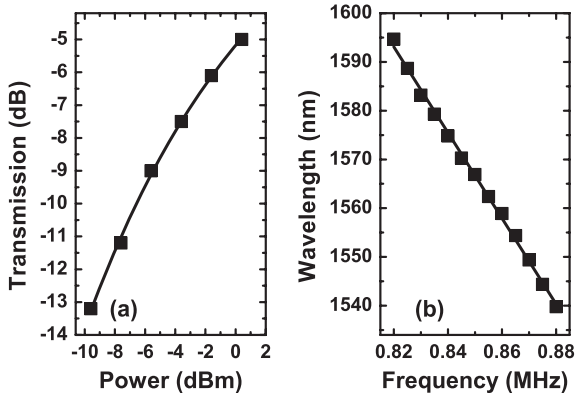

Fig. 3. (a) Bandpass coupling efficiency tunability and (b) central wavelength tunability of Port 3 from the tapered fiber.

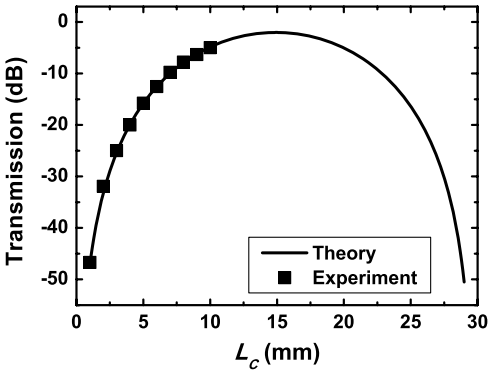

Fig. 4. The solid curve and solid squares denote the simulation and experimental results of the bandpass coupling efficiency as a function of L_C, respectively.

results agree with the theoretical prediction very well. Note that the maximally available coupling length L_C is 10 mm in our experiment, so there is still a large space to improve the bandpass coupling efficiency by increasing L_C. Besides, the bandpass coupling efficiency could also be improved, for example, by setting the uniform waist part of the tapered fiber to an appropriate diameter so that the cladding modes of the two fibers have similar effective index. Furthermore, the transition zone of the tapered fiber should be long enough and the diameter of the tapered fiber should vary slowly enough to decrease the coupling loss in the transition zone [10].

In conclusion, we have experimentally realized a tunable add/drop channel coupler based on an AOTF and a tapered fiber. The coupling efficiency and the central wavelength of the add/drop channels can be controlled by tuning the power and frequency of the driving RF signal applied to the AOTF. At the same time, possible improvements on the configuration are discussed. Combined with our recent fiber-winding AOTF structure in which multi-AOTFs are driven synchronously by one cuneal acoustic transducer [15], the tunable multichannel add/drop coupler can be fabricated. Such add/drop couplers are very useful for coarse WDM applications.

This work is supported by the 973 Program (2010CB934101), the Chinese National Key Basic Research Special Fund (2011CB922003), the International S&T Cooperation Program of China (2011DFA52870), the National Natural Science Foundation of China (90922030, 11174153, 10804054, and 10904077), the 111 Project (B07013), the Natural Science Foundation of Tianjin, the Cultivation Fund of the Key Scientific and Technical Innovation Project, Ministry of Education of China (708022), and the Fundamental Research Funds for the Central Universities.

References

1. H. A. Haus and Y. Lai, J. Lightwave Technol. **10**, 57 (1992).
2. B. Moslehi, P. Harvey, J. Ng, and T. Jannson, Opt. Lett. **14**, 1088 (1989).
3. J. L. Archambault, P. St. J. Russell, S. Barcelos, P. Hua, and L. Reekie, Opt. Lett. **19**, 180 (1994).
4. I. Baumann, J. Seifert, W. Nowak, and M. Sauer, IEEE Photon. Technol. Lett. **8**, 1331 (1996).
5. G. Meltz, W. W. Morey, and W. H. Glenn, Opt. Lett. **14**, 823 (1989).
6. K. S. Chiang, Y. Q. Liu, M. N. Ng, and S. P. Li, Electron. Lett. **36**, 1408 (2000).
7. Y. Q. Liu, K. S. Chiang, Y. J. Rao, Z. L. Ran, and T. Zhu, Opt. Express **15**, 17645 (2007).
8. A. M. Vengsarkar, P. J. Lemaire, J. B. Judkins, V. Bhatia, T. Erdogan, and J. E. Sipe, J. Lightwave Technol. **14**, 58 (1996).
9. Y. Q. Liu, Q. Liu, and K. S. Chiang, Opt. Lett. **34**, 1726 (2009).
10. A. P. Luo, K. Gao, F. Liu, R. H. Qu, and Z. J. Fang, Opt. Commun. **240**, 69 (2004).
11. Y. G. Han, S. B. Lee, C. S. Kim, and M. Y. Jeong, Opt. Lett. **31**, 703 (2006).
12. B. Y. Kim, J. N. Blake, H. E. Engan, and H. J. Shaw, Opt. Lett. **11**, 389 (1986).
13. H. S. Park, K. Y. Song, S. H. Yun, and B. Y. Kim, J. Lightwave Technol. **20**, 1864 (2002).
14. T. A. Birks and Y. W. Li, J. Lightwave Technol. **10**, 432 (1992).
15. W. D. Zhang, F. Gao, F. Bo, Q. Wu, G. Q. Zhang, and J. J. Xu, Opt. Lett. **36**, 271 (2011).
16. H. Li, T. Liu, C. Y. Wen, Y. C. Soh, and Y. Zhang, Opt. Eng. **42**, 3409 (2003).
17. K. S. Chiang, F. Y. M. Chan, and M. N. Ng, J. Lightwave Technol. **22**, 1358 (2004).